CEBAF-PR-89-036
WM-89-109

A Covariant Multiple Scattering Series for Elastic Projectile-Target Scattering

Frans Gross
Department of Physics, College of William and Mary
Williamsburg, VA 23185, USA
and
Continuous Electron Beam Accelerator Facility
12000 Jefferson Avenue, Newport News, VA 23606, USA

Khin Maung-Maung
Department of Physics, Hampton University
Hampton, VA 23668, USA
and
NASA Langley Research Center
Hampton, VA 23665, USA

CONTINUOUS

ELECTRON

BEAM

ACCELERATOR

FACILITY

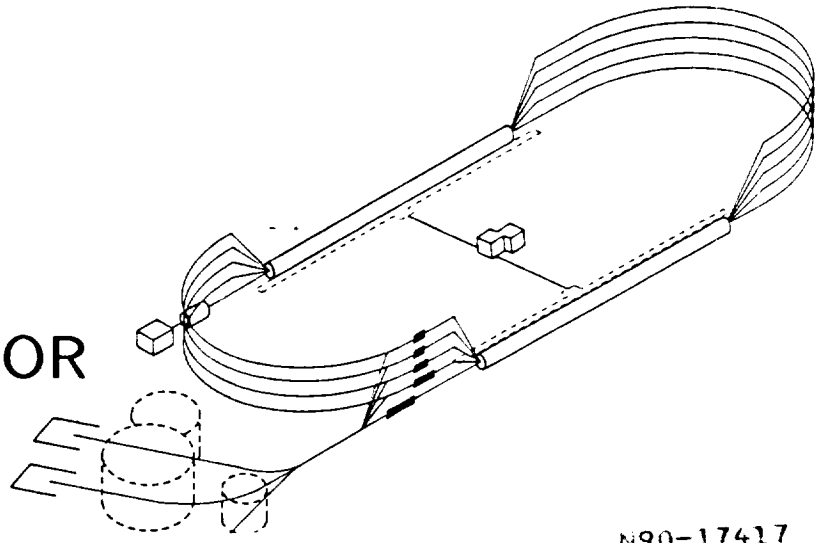

SURA SOUTHEASTERN UNIVERSITIES RESEARCH ASSOCIATION

CEBAF

Newport News, Virginia

Copies available from:

Library
CEBAF
12000 Jefferson Avenue
Newport News
Virginia 23606

The Southeastern Universities Research Association (SURA) operates the Continuous Electron Beam Accelerator Facility for the United States Department of Energy under contract DE-AC05-84ER40150.

A Covariant Multiple Scattering Series for Elastic Projectile-Target Scattering

by

Franz Gross
Department of Physics
College of William and Mary
Williamsburg, Virginia 23185
and
Continuous Electron Beam Accelerator Facility
Newport News, Virginia 23606

Khin Maung Maung
Department of Physics
Hampton University
Hampton, Virginia 23668
and
NASA Langley Research Center
Hampton, Virginia 23665

Abstract

A covariant formulation of the multiple scattering series for the optical potential is presented. We consider the case of a scalar "nucleon "interacting with a spin zero isospin zero A-body target through meson exchange. We show that a covariant equation for the projectile-target t-matrix can be obtained which sums the ladder and crossed ladder diagrams efficiently. From this equation, a multiple scattering series for the optical potential is derived, and we show that in the impulse approximation, the two-body t-matrix associated with the first-order optical potential is the one in which one particle is kept on mass-shell. The meaning of various terms in the multiple scattering series is given and we describe how to construct the first-order optical potential for elastic scattering calculations.

PACS numbers: 11.80.-m, 11.80.La, 24.10.Ht, 25.40.Cm

I. Introduction.

It is well known that the relativistic (Dirac equation) calculations give superior results to the non-relativistic (NR) calculations in the case of p-nucleus elastic scattering and have been widely used in recent calculations.[1,2] The first order optical potential used in these calculations is the relativistic impulse approximation (RIA)[1] which is a relativistic generalization of the non-relativistic $t\rho$ approximation. In the NR theory the elastic scattering of the projectile from the target nucleus is described by an effective interaction (optical potential) which is to be used in the Schrodinger equation, and the scattering observables are then obtained. The optical potential itself can be expressed as an infinite series of scattering terms, single, double etc, scatterings (hence the name multiple scattering series) in which there are no two successive scatterings from the same target particle. By keeping only the first term of the infinite series of the optical potential we obtain the first-order optical potential. The $t\rho$ approximation is achieved only after two more approximations, namely the impulse approximation which treats the struck target nucleon as though it were free, and the factorization approximation which assumes that the range of the interaction is small compared to the size of the nucleus. The last approximation is usually applied in order to avoid the complexities of performing the folding integral to obtain the optical potential. The existence of a multiple scattering series for the optical potential (in fact there are several in the literature) provides us with a means to calculate systematic corrections to the first-order results.

In the relativistic p-nucleus scattering calculations the effective one-body equation is taken to be the fixed energy Dirac equation. This choice is intuitively appealing as long as one considers the proton as an elementary fermion, but the actual validity of this assumption is still in question. This type of question will be answered only when one has the non-perturbative aspects of QCD under the same degree of control as in NR theories. Now the question arises as to what effective interaction (optical potential) should be used in the Dirac equation to describe p-nucleus scattering. As mentioned above, in all the relativistic calculations, the optical potential used has been the RIA.[1] The RIA optical potential is obtained by simply folding a relativistic NN amplitude with the nuclear density

matrix. Strictly speaking, use of the RIA is an intuitive guess guided by the non-relativistic multiple scattering formalism, since a relativistic multiple scattering theory (RMST) has not been available.

It is important to realize that without a multiple scattering theory the t-matrix associated with the first order optical potential cannot be unambiguously determined and consequently the characters of the corrections to be made to the first-order optical potential are not well defined. The absence of such a theory prevents us from making systematic corrections, such as Pauli blocking, in a consistent manner. Therefore it is highly desirable to have a RMST. Probably the most appropriate approach might be to apply the methods of field theory to the problem. But the development of the RMST in this direction has been hampered by the problems arising in the treatment of the interacting many-body ground state,[3] description of the residual interaction between the projectile particle and the target constituents, and many other obstacles not encountered in the NR theory.

In this work we take a less formal but more intuitive approach and describe the projectile nucleus scattering problem in a meson exchange model. A brief account of this work has already been given.[4] In this paper we will developed the ideas reported there in more detail.

From the beginning, we would like to make it clear that our aim is to derive a multiple scattering theory for the projectile nucleus scattering in the context of meson exchange. We will not consider the full implication of the formal field theoretical treatment of the interacting many-body problem, which is admittedly very difficult. We develop an approach which permits the standard multiple scattering techniques of NR theory to be applied with slight modification. We ignore the full complications of antisymmetry required by the Pauli principle and also ignore the spin part of the problem. We do not assume any particular form of equation for the projectile-nucleus t-matrix, but begin with the most obvious fact that the t-matrix is obtained by summing an infinite set of diagrams in which the projectile is interacting with the target particles through meson exchange. Although it seems much less complicated than the formal field theoretical approach it has its share of problems, such as the appearance of spurious singularities and the necessity for judicious treatment of the crossed meson diagrams. In this work we show how a RMST can be

formulated within the context of meson exchange, unambiguously determine the t-matrix associated with the optical potential, and show that under the impluse approximation the t-matrix to be used in the first-order optical potential is the solution of a relativistic two-body equation in which one particle is kept on its mass-shell.

This paper is arranged as follows. In section II the derivation of a multiple scattering series of the optical potential is reviewed, following the approach of Watson.[5] In section III.A it is shown how the crossed meson diagrams should be treated together with the box diagram for the case where the intermediate state target is in the ground state. In III.B the complications that arise in the case of intermediate target excited states are discussed, and it is shown how to handle the box and crossed box diagrams in this case. In subsection III.C a covariant equation for the projectile-target t-matrix is presented and it is shown how a multiple scattering series for the optical potential can be derived. The meaning of various terms in the multiple scattering series are discussed, and it is shown that the most appropriate two-body t-matrix to be used in the first-order optical potential under the impulse approximation is the one calculated from a covariant equation in which one particle is kept on the mass-shell. A general discussion and conclusion follows.

II. Non-relativistic Formalism.

In this section the non-relativistic multiple scattering formalism is reviewed. The approach of Watson[5] is followed, since it is more closely related to our relativistic formalism than the more commonly used KMT[6] method . Since we are interested in deriving a relativistic multiple scattering series for the optical potential, we will bypass the multiple scattering treatment of the t-matrix and will concentrate, in the present section, on the multiple scattering analysis[7] of the non-relativistic optical potential.

We begin with a total Hamiltonian H for the projectile-nucleus system given by

$$H = H_0 + V \tag{2.1}$$

with

$$H_0 = H_A + h_0 \tag{2.2}$$

and

$$H_A = \sum_{i=1}^{A} h_i + \sum_{i<j} v_{ij} \tag{2.3}$$

$$V = \sum_{i=1}^{A} v_i \tag{2.4}$$

Notice that the total Hamiltonian H is separated into two parts, the unperturbed Hamiltonian H_0 and the residual interaction V. It is the separability of H into H_0 and V, which permits the derivation of a multiple scattering formalism. The residual interaction V is taken to be the sum of the two-body interactions between the projectile particle "0 "and the target particle "i ". The unperturbed Hamiltonian H_0 is written as the sum of the target Hamiltonian H_A and h_0, the kinetic energy operator for the projectile . In NR formalism, the target Hamiltonian is just the kinetic energy operators of the target particles plus the sum of their pair interactions.

The separation of the total Hamiltonian in Eq(2.1) implies that we have some means in finding the solution to the target Hamiltonian H_A. Therefore in NR theory the complexities of the A-body problem are separated from the rest at the very beginning. Now write the Lippmann-Schwinger equation for the projectile-nucleus t-matrix in operator form as

$$T = V + VG_0T \tag{2.5}$$

with

$$G_0 = [E - H_0 + i\eta]^{-1} \tag{2.6}$$

Here G_0 is the unperturbed Greens function and the $i\eta$ prescription has been used to incorporate the outgoing boundary condition. The many-body nature of Eq(2.5) is apparent since the propagator G_0 involves the target Hamiltonian H_A.

For elastic scattering problems it is useful to introduce an effective one-body potential (optical potential). The optical potential is defined as the potential that describes the passage of a projectile through the nucleus with the nucleus treated as a passive medium i.e the nucleus is treated as though it cannot be excited. To accomplish this, first define a projection operator P which projects onto the ground state of the target and Q which

projects onto the excited states of the target including the break-up states. Therefore,

$$P + Q = 1 \tag{2.7}$$

where

$$P = |\phi_0 >< \phi_0| \tag{2.8}$$

and $|\phi_0>$ is the target ground state. Now Eq(2.5) can be rewritten as

$$T = U + UPG_0PT \tag{2.9}$$

$$U = V + VQG_0QU \tag{2.10}$$

The U appearing in these equations is the optical potential operator and Eq(2.9) together with Eq(2.10) are equivalent to Eq(2.5).

Since we are dealing with strong interactions, it is impractical to solve Eq(2.10) for U as it stands. It is at this point that the multiple scattering approach provides us with a big advantage. We may express U as $\sum_{i=1}^{A} U_i$ and rewrite Eq(2.10) as

$$U_i = v_i + v_iQG_0Q\sum_{j=1}^{A} U_j. \tag{2.11}$$

Now define the Watson τ operator as

$$\tau_i = v_i + v_iQG_0Q\tau_i \tag{2.12}$$

and observe that Eq(2.11) can be written in terms of τ

$$U_i = \tau_i + \tau_iQG_0Q\sum_{j\neq i} U_j. \tag{2.13}$$

Summing over the index i in the last equation gives the Watson multiple scattering series for the optical potential operator

$$U = \sum_{i=1}^{A} \tau_i + \sum_{i=1}^{A} \tau_iQG_0Q\sum_{j\neq i} U_j \tag{2.14}$$

Notice that Eq(2.14) is an infinite series in τ instead of the two-body interactions v as in Eq(2.10). Each term of Eq(2.14) can be interpreted as single scattering, double scattering and so on, hence the name multiple scattering series. By keeping only the first term of the series we obtain the first-order Watson optical potential

$$U^{1^{st}} = \sum_{i=1}^{A} \tau_i \tag{2.15}$$

The operator τ is not the free two-body t-matrix because of the many-body propagator in Eq(2.12), but related to it by

$$\tau = t + t(QG_0Q - g)\tau \tag{2.16}$$

where the free two-body t-matrix is defined as

$$t = v + vgt \tag{2.17}$$

with g the free two-body propagator. For high projectile incident energies one usually approximates τ by t (impluse approximation[7]) and obtains for the first-order Watson impluse approximation optical potential

$$U_{Im}^{1^{st}} = \sum_{i=1}^{A} t_i \tag{2.18}$$

We can also rewrite Eq(2.14) in terms of the free two-body t-matrix, t

$$U = \sum_i t_i + \sum_i t_i(QG_0Q - g)U_i + \sum_{i \neq j} t_i QG_0 QU_j \tag{2.19}$$

As we have mentioned above the first term in Eq(2.19) gives the first-order impulse approximation optical potential. The second term can be interpreted as the propagator correction term. This term originates from the fact that we have written the optical potential in terms of the free t-matrix t instead of τ. For high projectile energies the differences between t and τ become negligible and the impulse approximation should give good results. The last term represents the multiple scattering terms. For NR scattering calculations the t-matrix appearing in Eq(2.19) can be obtained from Eq(2.17) by employing a choice of v,

for example the Reid potential, or by fitting the NN experimental data directly by using an appropriate functional form. After the choice for the t-matrix is made, solving Eq(2.17) together with Eq(2.9) is just a technicality.

III. Relativistic Formalism

In the last section we reviewed the non-relativistic multiple scattering formalism and outlined how a multiple scattering series for the optical potential can be obtained. We pointed out that the key feature that enables us to construct a multiple scattering series is the separability of the total Hamiltonian into an unperturbed Hamiltonian describing the free projectile-target system and the residual interaction which is the sum of the two-body interactions between the projectile and the target particles. Unfortunately, there is no analogous procedure in the relativistic case. First of all, one cannot naively write the target Hamiltonian as the sum of the Dirac Hamiltonians plus the sum of two-body interactions, since the Hamiltonian written in this manner does not have a lower bound.[3] In order to treat the projectile target scattering consistently in a relativistic formalism one needs to resort to a field theoretical approach.

In this work we take a less ambitious route and show that a relativistic multiple scattering series can be formulated in the context of a relativistic meson exchange model. In the following we will consider a scalar "nucleon "interacting with an A-body spin zero iso-spin zero target where the interaction between the projectile and the target is described by meson exchange. Since we do not assume any particular form of equation for the projectile target t-matrix, we will start from the most obvious fact that it can be obtained by summing all possible meson exchange diagrams of the projectile target system. A minimal set of meson exchange diagrams required for any such theory is the set of ladder and crossed ladder diagrams. In the limit when the heavy target becomes infinitely massive, this set reduces to a one-body equation for the lighter particle moving in an instantaneous potential produced by the heavier particle (the one body limit[8]), and at high energies gives the eikonal approximation to scattering[9]. In this work we seek a theory in which these relativistic ladder and crossed ladder diagrams are summed efficiently.

In Fig.1 the target is represented by a double line, the dash lines represent the exchanged particle (meson) and the solid line represents the projectile. For the intermediate states the target can be in its ground state, denoted by $n = 0$, or in excited states, $n \neq 0$, which includes the break-up states. The notation is very compact; each diagram in Fig.1 actually represents a set of diagrams which can be obtained by opening up the bubbles at the meson-target vertices. For example the set of diagrams contained in the box, Fig.1b and crossed-box, Fig.1c diagrams are shown explicitly in Figs 2 and 3.

In our view, the solution of the relativistic problem in the meson exchange approximation is equivalent to finding an integral equation which sums all of the diagrams shown in Fig.1. The construction of such an equation confronts us with three problems. The first problem, which does not occur in the non-relativistic case, is the appearance of the crossed meson diagrams. These and all other irreducible diagrams (i.e those which cannot be separated in to two pieces by a line which intersects only the projectile and the target) will be included in the kernel of the integral equation. The second problem concerns the treatment of excited states. All diagrams, except for the one meson exchange term, include terms in which the target propagates in an excited state. A third problem is that each diagram includes terms in which the projectile may interact with two or more different target particles (multiple scattering). In this section, we will first discuss how the crossed diagrams are handled, and then discuss the complications arising from the occurance of excited states.

A. Cancellation between the Box and Crossed Box diagrams.

We know from the two-body problem that the ladder sum does not give a good approximation to the true solution of the Bethe-Salpeter equation. There is no reason to believe that it would be otherwise here. In fact, in the two-body problem the box diagram and the crossed box diagram tend to cancel, showing that it is unjustified to neglect crossed meson diagrams.

In this section we show that the cancellations between the box diagram and the cross-box diagram still occur in the case of projectile nucleus scattering. In order to demonstrate this cancellation, we perform the integration over the relative energy for the intermediate

states.

In Fig.4 the box diagram, Fig.1b, and the crossed box diagram, Fig.1c, are redrawn and the 4-momentum variables for each internal particle are labeled. For our purpose now, it is sufficient to consider the target as a structureless particle as shown in Fig.4. By employing standard Feynman rules the box and crossed box diagrams of Fig.4 are given by the following expressions.

$$M^{(4A)} = \frac{ig^4}{(2\pi)^4}\int \frac{d^3k'dp'_0[\omega^2-(e(\mathbf{k})-p'_0)^2-i\eta]^{-2}}{[e^2(\mathbf{k}')-p'^2_0-i\eta][E_n^2(\mathbf{k}')-(W-p'_0)^2-i\eta]} \tag{3.1}$$

$$M^{(4B)} = \frac{ig^4}{(2\pi)^4}\int \frac{d^3k'dp'_0[\omega^2-(e(\mathbf{k})-p'_0)^2-i\eta]^{-2}}{[e^2(\mathbf{q}')-(2e(\mathbf{k})-p'_0)^2-i\eta][E_n^2(\mathbf{k}')-(W-p'_0)^2-i\eta]} \tag{3.2}$$

where the total four momenta in the c.m is

$$p + P = (W,0) = p' + P' = p'' + P''$$

and the three momenta and the on-shell energies are defined as

$$\mathbf{p} = -\mathbf{P} = \mathbf{k} \; ; \; \mathbf{q} = \mathbf{p} - \mathbf{p}' + \mathbf{p}'' \; ; \; \mathbf{p}' = -\mathbf{P}' = \mathbf{k}'$$

$$\omega = (\mu^2 + (\mathbf{k}'-\mathbf{k})^2)^{1/2} \; ; \; e(\mathbf{k}) = (m^2+\mathbf{k}^2)^{1/2} \; ; \; E_n(\mathbf{k}) = (M_n^2+\mathbf{k}^2)^{1/2}$$

We assume forward scattering, i.e $\mathbf{k} = \mathbf{k}''$, so that the meson poles become double poles. The external particles are taken to be on their mass-shell.

Figure 5a and 5b show the locations of the poles (when $|\mathbf{k}|$ and $|\mathbf{k}'|$ are small) for the box diagram and crossed box diagram, respectively. We will evaluate the box and crossed box diagrams by using the residue theorem. In the following expressions the superscript on M distinguishes between the box and the crossed box diagrams, the subscript is for the type of pole under consideration, and the letters U(upper half plane) and L(for lower half plane) are used to remind us how the contour is closed. For example $M^{4A}_{-p}(U, n=0)$ means the negative energy projectile pole (-p) contribution from the fourth-order box diagram (4A) for $n = 0$, and the integration contour is closed in the upper half plane.

Evaluate the box diagram for $n = 0$. Close the contour in the upper half plane and pick up the target positive energy pole, double meson pole and the projectile negative pole.

$$M^{4A}(U,n=0) = M^{4A}_{+T}(U,n=0) + M^{4A}_{\pi}(U,n=0) + M^{4A}_{-p}(U,n=0)$$

where we have used the sub-script π suggestively for the meson double pole contribution. These contributions are

$$M^{4A}_{+T}(U,n=0) = -\frac{g^4}{(2\pi)^3}\int \frac{d^3k'[\omega^2-(E_o(\mathbf{k}')-E_o(\mathbf{k}))^2]^{-2}}{[2E_o(\mathbf{k}')][e^2(\mathbf{k}')-(e(\mathbf{k})+E_o(\mathbf{k})-E_o(\mathbf{k}'))^2]}$$

$$M^{4A}_{\pi}(U,n=0) = -\frac{g^4}{(2\pi)^3}\int \frac{d^3k'[A-B]}{4\omega^3[e^2(\mathbf{k}')-(e(\mathbf{k})-\omega)^2]^2[E_o^2(\mathbf{k}')-(E_o(\mathbf{k})+\omega)^2]^2}$$

$$M^{4A}_{-p}(U,n=0) = -\frac{g^4}{(2\pi)^3}\int \frac{d^3k'}{[\omega^2-(e(\mathbf{k})+e(\mathbf{k}'))^2[2e(\mathbf{k}')][E_o^2(\mathbf{k}')-(W+e(\mathbf{k}'))^2]}$$

where

$$A = [E_o^2(\mathbf{k}')-(E_o(\mathbf{k})+\omega)^2]\{[e^2(\mathbf{k}')-(e(\mathbf{k})-\omega)^2]+2\omega(e(\mathbf{k})-\omega)\}$$

$$B = 2\omega(E_o(\mathbf{k})+\omega)[e^2(\mathbf{k}')-(e(\mathbf{k})-\omega)^2]$$

For the crossed box diagram we close the contour in the lower half plane for all n and pick up the double meson poles and negative energy projectile and target poles.

$$M^{4B}(L,n) = M^{4B}_{\pi}(L,n)+M^{4B}_{-p}(L,n)+M^{4B}_{-T}(L,n)$$

The individual pole contributions are

$$M^{4B}_{\pi}(L,n) = -\frac{g^4}{(2\pi)^3}\int \frac{d^3k'[F+G]}{4\omega^3[e^2(\mathbf{q})-(e(\mathbf{k})-\omega)^2]^2[E_n^2(\mathbf{k}')-(E_o(\mathbf{k})-\omega)^2]^2}$$

$$M^{4B}_{-p}(L,n) = -\frac{g^4}{(2\pi)^3}\int \frac{d^3k'}{[\omega^2-(e(\mathbf{k})+e(\mathbf{q}))^2]^2[2e(\mathbf{q})][E_n^2(\mathbf{k}')-(E_o(\mathbf{k})-e(\mathbf{k})-e(\mathbf{q}))^2]}$$

$$M^{4B}_{-T}(L,n) = -\frac{g^4}{(2\pi)^3}\int \frac{d^3k'[\omega^2-(E_o(\mathbf{k})+E_n(\mathbf{k}'))^2]^{-2}}{[e^2(\mathbf{q})-(e(\mathbf{k})-E_o(\mathbf{k})-E_n(\mathbf{k}'))^2][2E_n(\mathbf{k}')]}$$

where

$$F = [E_n^2(\mathbf{k}')-(E_o(\mathbf{k})-\omega)^2]\{[e^2(\mathbf{q})-(e(\mathbf{k})-\omega)^2]+2\omega(e(\mathbf{k})-\omega)\}$$

$$G = 2\omega(E_o(\mathbf{k})-\omega)[e^2(\mathbf{q})-(e(\mathbf{k})-\omega)^2]$$

At this stage one could show that, at threshold, the dominant contribution of the box diagram for $n=0$ comes from the positive energy target pole and the meson poles give the

second largest contribution. For the crossed box diagram, the meson pole contribution is the dominant one and is nearly equal to the meson pole contribution from the box diagram but with a relative negative sign. Since we are interested in other energies beside threshold, we evaluate the various pole contributions without any further approximations. The only restriction is forward scattering.

Figure 6 demonstrates the cancellation between the box diagram and the crossed box diagram. The dashed line is $|(M^{4A}_{-p} + M^{4A}_{\pi})/M^{4A}_{+T}|$, the absolute magnitude of the ratio of the sum of negative energy projectile pole and meson pole contribution to the positive energy target pole contribution for $n = 0$. The dotted line is the ratio of all the pole contributions from the crossed box to the positive energy target pole of the box diagram. These two lines lie practically on top of each other. Finally, the solid line is $|(M^{4A}_{-p} + M^{4A}_{\pi} + M^{4B})/M^{4A}_{+T}|$ which is the ratio of the sum of the full crossed box and negative energy projectile pole plus the meson poles of the box diagram to the positive energy pole of the box diagram. In these calculations, the target mass is taken to be $M_0 = 16m$, where m is the mass of the projectile particle and the meson mass is taken to be $\mu = m/7$. This figure shows that, when the target is in the ground state ($n = 0$), the poles of the box diagram, which remain after the target is put on-shell, and the crossed box diagram, are each of the order of $10 - 30\%$ of the leading M^{4A}_{+T} term, and hence are far from being negligible. However, when the box and crossed box are taken together, an excellent cancellation occurs, as shown by the solid line for the energy range shown. After the cancellation, the positive energy target pole clearly dominates, and whatever is left over is less than 0.3% of this dominant contribution.

If the projectile is put on mass-shell, instead of the target, the ratio of the correction from the box and the crossed box to the leading term would be $|(M^{4A}_{-T}+M^{4A}_{\pi}+M^{4B})/M^{4A}_{+p}|$, and this is the dotdashed line shown in Fig.6. This result shows that the cancellation between the box and crossed box diagrams is not as complete when the projectile is on-shell, but still quite good. The terms which remain are now between $1 - 4\%$ of the leading term, an order of magnitude larger, then when the target is on-shell.

Figure 7 shows the A dependence of these cancellations. The legend of the curves mean the same as in Fig.6, but they are shown as functions of the target mass $M_0 = Am$,

where the binding energy is neglected. The projectile lab kinetic energy is fixed at 1 GeV. As can be seen from the solid line, if the target is on-shell the cancellations become better as A increases, and exact cancellation occurs when $A \to \infty$. As shown by the solid line, this is an excellent approximation even for light nuclei. If the projectile is on-shell the cancellation does not improve as $A \to \infty$, reflecting the fact that, in this case, the cancellation depends on the properties of the projectile and not on the target.

The above results suggest that, when the target is in the ground state, it is an excellent approximation to keep only the positive energy target pole for the intermediate states, which is equivalent to keeping the ground state target on its mass-shell in all intermediate states. The cancellation is less complete and the approximation less accurate for realistic cases with spin and charge exchange, so that it is desirable, in the general case, to include (at least in principle) these extra terms as higher order corrections to the kernel (they become part of $\hat{V}'$ in Eq.(3.5) as described below).

The alternative approach of putting the projectile on shell has been seen to be less well justified; the additional correction terms are larger and do not decrease as $A \to \infty$. We believe that this analysis provides a satisfactory motivation for using a fixed energy Dirac equation, in which the projectile is off-shell and the target is on-shell, to describe elastic nucleon-nucleus scattering.

B. Treatment of the Excited states

In this subsection we will consider how to treat the intermediate target excited states. It would be tempting to say that the same approximation that we have advocated in the case of $n = 0$ should work here also, and that the excited state of the target should be put on mass-shell. But for $n \neq 0$, further complications may arise because of the so called dissolution singularities.[10]

The dissoulution singularities are spurious singularities which arise when a highly excited heavy target is put on its mass-shell. To see how they come about, consider putting the excited target on its mass-shell in the expression for the box diagram i.e

$$[E_n^2(\mathbf{k}') - (W - p'_0)^2 - i\eta]^{-1} \to 2\pi i \frac{\delta(p'_0 - (W - E_n(\mathbf{k}')))}{2E_n(\mathbf{k}')}$$

The projectile propagator in Eq(3.1) can be factorized into

$$[e^2(\mathbf{k}') - p'^2_0]^{-1} = [e(\mathbf{k}') + (W - E_n(\mathbf{k}'))]^{-1}[e(\mathbf{k}') - (W - E_n(\mathbf{k}'))]^{-1}$$

In the last expression we see that there are two singularities, one at $W = e(\mathbf{k}') + E_n(\mathbf{k}')$ which is the usual elastic cut and the other one at $W = E_n(\mathbf{k}') - e(\mathbf{k}')$ which is the dissolution singularity. This second singularity is spurious because it does not occur when the diagram is calculated exactly. (It can be shown that it is cancelled by a similar singularity in the M^{4A}_{-p} term.) When $n = 0$, this singularity occurs at $W = E_0 - e$, which is way below threshold and hence not of importance. However, when the intermediate state is highly excited ($n \neq 0$), the singularity can move into the physical region and is a cause for concern. It has been an obstacle in developing a RMST.

To see when this singularity becomes potentially dangerous, study the locations of the poles in the box diagram, Fig.5a. By approximating $W \approx M_0 + m$ (threshold) and taking $|\mathbf{k}'|$ to be small so that $e(\mathbf{k}') \approx m$ and $E_n(\mathbf{k}') \approx M_n$, we see that the negative energy projectile pole and the positive energy target pole are separated by an amount $M_0 - M_n + 2m$ in the upper half plane. As M_n increases, the positive energy target pole moves towards the negative energy projectile pole and when the excitation energy of the target reaches $2m$ the poles touch and a singularity arises. In this situation it is clearly not a good approximation to take one of these poles and "neglect "the other. In addition to these spurious singularities in the projectile propagator, there are other spurious singularities arising from the meson propagators when the excited state target is put on its mass-shell. For calculational purposes these meson singularities are even worse than the ones from the projectile propagator since they can arise for relatively low excitation energies. At threshold they will appear when the excitation energy reaches the meson mass.

The situation in the lower half plane (Fig 5a) is different. As E_n increases the negative energy target pole moves away from the positive energy projectile pole. To see this explicitly we put the projectile on its mass-shell in Eq(3.1):

$$[e^2(\mathbf{k}') - p'^2_0]^{-1} \rightarrow 2\pi i \frac{\delta(p'_0 - e(\mathbf{k}'))}{2e(\mathbf{k}')}$$

and the target propagator is now

$$[E_n^2(\mathbf{k}') - (W - p'_0)]^{-1} = [E_n(\mathbf{k}') - (W - e(\mathbf{k}'))]^{-1}[E_n(\mathbf{k}') + (W - e(\mathbf{k}'))]^{-1}$$

and exhibits no spurious singularities in the physical region. It can easily be seen that meson propagators do not have any such singularities either.

The above analysis suggests that, when we evaluate the expression (3.1) for $n = 0$, we should close the contour in the upper half plane (to obtain the best approximation), but for $n \neq 0$ we should close the contour in the lower half plane to eliminate the problem of spurious singularities.

We now study the accuracy of this prescription by evaluating the box diagram for $n \neq 0$ by closing the contour in the lower half plane. The contributions come from the positive energy projectile pole, double meson pole and negative energy target pole.

$$M^{4A}(L, n \neq 0) = M^{4A}_{+p}(L, n \neq 0) + M^{4A}_{\pi}(L, n \neq 0) + M^{4A}_{-T}(L, n \neq 0)$$

The contribution from these poles is

$$M^{4A}_{+p}(L, n \neq 0) = -\frac{g^4}{(2\pi)^3} \int \frac{d^3k'}{[\omega^2 - (e(\mathbf{k}) - e(\mathbf{k}'))^2]^2[2e(\mathbf{k}')][E_n^2(\mathbf{k}') - (W - e(\mathbf{k}'))^2]}$$

$$M^{4A}_{-T}(L, n \neq 0) = -\frac{g^4}{(2\pi)^3} \int \frac{d^3k'}{[\omega^2 - (E_o(\mathbf{k}) + E_n(\mathbf{k}'))^2]^2[e^2(\mathbf{k}') - (W + E_n(\mathbf{k}'))^2][2E_n(\mathbf{k}')]}$$

$$M^{4A}_{\pi}(U, n \neq 0) = -\frac{g^4}{(2\pi)^3} \int \frac{d^3k'[C + D]}{4\omega^3[e^2(\mathbf{k}') - (e(\mathbf{k}) + \omega)^2]^2[E_n^2(\mathbf{k}') - (E_o(\mathbf{k}) - \omega)^2]^2}$$

where

$$C = [E_n^2(\mathbf{k}') - (E_o(\mathbf{k}) - \omega)^2]\{[e^2(\mathbf{k}') - (e(\mathbf{k}) + \omega)^2] - 2\omega(e(\mathbf{k}) + \omega)\}$$

$$D = 2\omega(E_o(\mathbf{k}) - \omega)[e^2(\mathbf{k}') - (e(\mathbf{k}) + \omega)^2]$$

In Fig.8 calculations of the $n \neq 0$ cases are shown. The dash line is the ratio of the sum of the meson poles(box) and target negative energy pole(box) to the positive

energy projectile pole(box) i.e $|(M^{4A}_{-T} + M^{4A}_{\pi})/M^{4A}_{+p}|$. The dotted line shows the ratio of the crossed box diagram to the positive energy pole of the box diagram. The solid line is $|(M^{4B} + M^{4A}_{-T} + M^{4A}_{\pi})/M^{4A}_{+p}|$ which is the ratio of the sum of the full crossed box and the negative target pole(box) plus meson poles(box) to the positive energy projectile pole. For this calculation the target mass and the meson mass are the same as the $n = 0$ case, and the excitation energy of the target is taken to be $\Delta m = m/100$. As in the $n = 0$ case, the cancellations between the box and the crossed box still occur to a very large extent, although the cancellation is not as good as in the previous case. It can be seen that, after the cancellation, the leftover terms in the energy range shown are less than 4% of the dominant projectile positive energy pole contribution.

In Fig.9 the curves mean the same as in Fig.8, but are shown as the function of target excitation energy with the projectile lab kinetic energy fixed at 1 GeV. As before the solid line shows the net result and it is seen that the cancellation becomes better as the excitation energy increases. This is a good signature, since as the excitation energy becomes higher, the one particle knockout term, which is the dominant inelastic contribution at medium energies, will become more important, and it is advantageous to have the cancellations improve as these contributions become larger.

The above analysis suggests that for the intermediate target excited states, keeping the positive energy projectile pole of the box diagram provides us with a very good approximation and at the same time avoids the spurious singularities that would arise by putting the excited target on the mass-shell.

C. Multiple Scattering Series for the Optical Potential.

In the above subsections, we have discussed the cancellations between the box and the crossed box diagrams for both $n = 0$ and $n \neq 0$. We have concluded that, because of the excellent cancellations between these diagrams, we should keep the target on the mass-shell for $n = 0$, and that for $n \neq 0$ we can avoid spurious singularities and still have a very good approximation if the projectile is kept on mass-shell. Note that these approximations are obtained by considering the box and crossed box together. If one considered the box diagram only, these approximations would not be as good, as can be seen by the dashed

curves of Figs 6 and 8.

We now follow the suggestion provided by the last two subsections and write an integral equation for the projectile-target t-matrix in the following form:

$$\hat{T} = \hat{V} + \hat{V} P G^T_{n=0} P \hat{T} + \hat{V} Q G^P_{n\neq 0} Q \hat{T} \tag{3.3}$$

where $G^T_{n=0}$ is the propagator for the target in its ground state and on its mass-shell, $G^P_{n\neq 0}$ is the propagator for the target in its excited states with the projectile on mass-shell, and P and Q are target ground state and excited state projection operators, respectively. $\hat{V}$ is the sum of all irreducible meson exchange contributions, where *now* all diagrams, or parts of diagrams, which do *not* have the target on mass-shell when $n = 0$, or the projectile on mass-shell when $n \neq 0$, are irreducible. This means that $\hat{V}$ is now the sum of all one meson exchange contributions between the projectile and the target (with target on mass-shell if $n = 0$ and projectile on mass-shell if $n \neq 0$) *plus* the crossed meson exchange diagrams *and* contributions from ladder diagrams coming from meson and negative energy poles. This definition of $\hat{V}$ is illustrated in Fig. 10. Since these latter terms tend to cancel (we demonstrated this only to 4^{th} order in the previous section, but we believe it to be true also to higher orders), $\hat{V}$ is well approximated by one meson exchange diagrams only.

Equation (3.3) is the first major result of this paper. It is a three dimensional covariant equation for the projectile-target t-matrix. If the irreducible diagrams are neglected the driving term of this equation, $\hat{V}$, assumes a very simple form. It is the sum of one meson exchanges between the projectile and the target particles. The special feature of this equation is that it has two three dimensional propagators in which the target is on mass-shell when the target is in the ground state and the projectile is on mass-shell when the target is in an excited state.

In the following we will show how a multiple scattering series for the optical potential that corresponds to Eq(3.3) can be obtained. By employing the projection operator method, we can rewrite Eq(3.3) as coupled equations:

$$\hat{T} = \hat{U} + \hat{U} P G^T_{n=0} P \hat{T} = \hat{U} + \hat{T} P G^T_{n=0} P \hat{U} \tag{3.4a}$$

$$\hat{U} = \hat{V} + \hat{V} Q G^P_{n\neq 0} Q \hat{U} = \hat{V} + \hat{U} Q G^P_{n\neq 0} Q \hat{V} \tag{3.4b}$$

Here $\hat{U}$ is our optical potential operator and we seek a multiple scattering series expression for this operator. It should be noted that Eqs(3.4) are three-dimensional equations. The first one Eq(3.4a) is the effective one-body equation for the projectile, and for a fermion projectile it becomes the fixed energy Dirac equation.

A multiple scattering series for the optical potential will be derived in a manner very similar to the NR theory. First write $\hat{V}$ as

$$\hat{V} = \sum_i \hat{v}_i + \hat{V}' \tag{3.5}$$

Where $\hat{v}_i$ are the one meson exchange diagrams describing the interaction of the projectile and the i^{th} nucleon of the target and $\hat{V}'$ is the sum of all the irreducible diagrams described above.

Next, as in the NR theory, we write $\hat{U} = \sum_i \hat{U}_i$ and obtain

$$\sum_i \hat{U}_i = \sum_i (\hat{v}_i + \hat{V}_i') + \sum_{i,j} (\hat{v}_i + \hat{V}_i') G^p_{n\neq 0} \hat{U}_j \tag{3.6}$$

We have defined $\hat{V}_i' = \hat{V}'/A$. In the above equation, and in the following, the projection operators P and Q are suppressed. It is to be understood that P goes with $G^T_{n=0}$ and Q goes with $G^p_{n\neq 0}$. Adding and subtracting the quantity $\sum_i \hat{v}_i g \hat{U}_i$ and dropping the sum over i gives

$$\hat{U}_i = \hat{v}_i + \hat{v}_i g \hat{U}_i + \sum_j \hat{v}_i (G^p_{n\neq 0} - g\delta_{ij}) \hat{U}_j + \hat{V}_i' + \sum_j \hat{V}_i' G^p_{n\neq 0} \hat{U}_j \tag{3.7}$$

where we have introduced a new propagator g whose properties are not specified at this stage. Taking the second term on the RHS of Eq(3.7) to the LHS and operating from the left with the inverse of $(1 - \hat{v}_i g)$ gives

$$\hat{U}_i = \bar{t}_i + \sum_j \bar{t}_i (G^p_{n\neq 0} - g\delta_{i,j}) \hat{U}_j + \bar{v}_i (1 + \sum_j G^p_{n\neq 0} \hat{U}_j)$$

where we have defined $\bar{t}_i$ and $\bar{v}_i$ as

$$\bar{t}_i = \hat{v}_i + \hat{v}_i g \bar{t}_i \tag{3.8}$$

$$\bar{v}_i = \hat{V}_i' + \hat{v}_i g \bar{v}_i \tag{3.9}$$

Resumming over the index i gives

$$\hat{U} = \sum_i \bar{t}_i + \sum_i \bar{t}_i (G^p_{n\neq 0} - g)\hat{U}_i + \sum_{i\neq j} \bar{t}_i G^p_{n\neq 0} \hat{U}_j + \sum_i [\bar{v}_i (1 + \sum_j G^p_{n\neq 0} \hat{U}_j)] \tag{3.10}$$

Equation (3.10) is our multiple scattering series for the optical potential, and it is the second major result of this paper. It should be compared with the NR analogue Eq(2.19).

The first term of this series can be interpreted as the single scattering term for the optical potential. The second term is the propagator correction term which obviously depends on our choice of the propagator g. The third term on the RHS of (3.10) corresponds to multiple scattering corrections and they are directly related to two, three etc. particle correlations and can be assumed to be small in the first approximation. The last term includes iterations of the irreducible diagrams with the one meson exchange terms. As previously explained, the contributions from these diagrams are small compared to the ones that we have kept, and are negligible in the first approximation.

Keeping the first term only gives a single scattering approximation for the optical potential. The propagator g has not yet been specified. In principle, one could use any convenient t-matrix for the $\bar{t}$ operator in Eq(3.10) as long as we are willing to incorporate the corrections represented by the rest of the terms in Eq(3.10). In practice one usually keeps only the first term of the series and the judicious choice of g is then essential.

Under normal conditions, the second term gives the largest correction to the single scattering approximation, and we therefore should pay the greatest attention to this term. We would like to choose our propagator g so that this correction is minimal. This can be accomplished by choosing the propagator g as shown in Fig.11 . In this figure, both the heavy $A-1$ cluster and the projectile are kept on their mass-shell.[11] In the medium energy range the terms represented by the sum $\sum \bar{t}_i Q G^p_{n\neq 0} Q \bar{t}_i$ are dominated by the one nucleon knockout term and our choice of g described above would exactly cancel these dominant inelastic contributions and ensure that they are exactly accounted for in the t-matrix itself given by Eq(3.8). Restricting the $A-1$ cluster to the mass-shell ensures cluster separability of the remaining two-nucleon system.[12]

With this choice of g, Eq(3.8) for $\bar{t}_i$ in the NN subspace reduces to the one particle on mass-shell (spectator) equation previously introduced by one of us.[13] The projection of $\bar{t}_i$ onto this subspace will be denoted by t_i. The only difference between t_i and the free two-body t-matrix is the shift in the total energy of the two-body subspace due to the motion of the free $A-1$ cluster. In analogy with the NR theory, this choice of g can be viewed as the "Impluse Approximation "choice of g in our theory. The spectator Eq(3.8) is shown diagrammatically in Fig.12.

We conclude that the most appropriate t-matrix to be used in the optical potential should be calculated from a covariant three-dimensional equation for two particles in which one particle is kept on its mass-shell. This choice will minimize the leading correction to the multiple scattering series Eq(3.10).

The last step is to carry out the necessary projections to obtain final equations for elastic scattering in the impulse approximation. The elastic scattering scattering amplitude is $T = P\hat{T}P$, which satisfies the equation

$$T = U + UG_{n=0}^{T}T \tag{3.11}$$

where $U = P\hat{U}P$. Equation (3.11) is just the projection of Eq(3.4a). In the single scattering approximation,

$$\hat{U} = \sum_i \bar{t}_i \tag{3.12}$$

where $\bar{t}_i$ is the operator satisfying (3.8), or alternatively,

$$\bar{t}_i = \hat{v}_i + \bar{t}_i g \hat{v}_i \tag{3.8b}$$

Using both (3.8) and (3.8b) we obtain an alternative equation for $\bar{t}_i$

$$\bar{t}_i = \hat{v}_i + \hat{v}_i g \hat{v}_i + \hat{v}_i g \bar{t}_i g \hat{v}_i \tag{3.13}$$

If we define $v_i(t_i)$ to be the projection of $\hat{v}_i(\bar{t}_i)$ on to the subspace of states connected to g, the first-order optical potential in the impulse approximation is finally obtained as

$$U_{IA}^{1st} = \sum_i P\bar{t}_i P = \sum_i [P\hat{v}_i P + P\hat{v}_i g \hat{v}_i P + P\hat{v}_i g t_i g \hat{v}_i P] \tag{3.14a}$$

where

$$t_i = v_i + v_i g t_i = v_i + t_i g v_i \tag{3.14b}$$

Note that (3.14b) is equivalent to the two-boby equation with the projectile on shell, as described above and illustrated in Fig.12 and (3.14a) tells how all four legs of this two-body t-matrix are extrapolated off-shell for use in the optical potential. Note that $\bar{t}_i$, has all four legs off-shell (and includes a delta function in the $A-1$ spectator coordinates), but is identical to t_i if one particle is on-shell in the initial and final state (and the delta finction in the $A-1$ coordinates is dropped). Furthermore, no further equation must be solved to obtained it; it is obtained directly from t_i by quadrature; Eq(3.14a). Equation (3.14a) is illustrated in Fig.13; its 4^{th} order contribution was already encountered in one of the terms in Fig.2.

IV. Discussion and Conclusion

In this paper we have considered a covariant formalism for projectile-target scattering in the context of meson exchange, and have shown that a multiple scattering series for the optical potential can be derived. We do not claim that we have derived a RMST starting from a field theoretical Lagrangian, but we do claim that we have derived a multiple scattering theory in a covariant manner. Every step of our derivation is manifestly covariant and the end result, the t-matrix associated with the impulse approximation optical potential, must also be calculated from a relativistically covariant equation.

In conclusion, we will restate what we have accomplished in this paper. In the context of meson exchange we have derived a covariant equation for the projectile nucleus t-matrix Eq(3.3). This equation was derived by considering the cancellations between the box and crossed box diagrams and we have also shown how the spurious singularities can be avoided. We then derived a multiple scattering series for the optical potential and showed, in the impulse approximation, that the t-matrix associated with the optical potential is to be calculated from a relativistic three dimensional equation in which one particle is kept on its mass-shell. We also described how the fully off-shell extension of this t-matrix Eq(3.8) can be calculated from a quadrature, Eq(3.14a). We emphasize that our development

leads to a precise definition of the t-matrix to be used in the impluse approximation of the first-order optical potential. This is the principal difference between our result and the RIA as commonly used. The t-matrix is to be obtained from a one-particle on mass-shell equation. Hence intermediate states with both nucleons in negative energy states can not occur, except at the "end points ", as illustrated in Fig.13. This result is obtained from a careful analysis of meson exchange diagrams, and seems to be the most appropriate for the problem of elastic nucleon-nucleus scattering. Numerical tests support this approach. It has been found that the contributions from channels in which both nucleons are in negative energy states is negligible.[14] The amplitudes calculated from Eq(3.14b) have been used in an analysis of $p-^{40}Ca$ elastic scattering[14,15], and excellent agreement with experimental data has been obtained. Differences between ours and that of Tjon and Wallace[1] were visible, but not large.

Since our first order impluse approximation optical potential is derived from a multiple scattering theory, it is possible to make systematic corrections to the first order calculations. We first intend to calculate the four leg off-shell t-matrix from the quadrature equation Eq(3.14a) and then evaluate other corrections. For example the double scattering correction term can be calculated in a straight forward manner as in the NR theory. Calculation of two-particle correlation functions, in a relativistically consistent manner, will be an obstacle. In the first approximation, one could treat the excited state target as a nonrelativistic object and neglect the small contributions from the negative energy propagation. In this approximation the second order (double scattering terms) in the expansion of the optical potential can be calculated in a standard manner by employing the t-matrix obtained from the spectator equation.

Finally we point out that we have not considered the problem of antisymmetry between the projectile and the target particles, nor the self consistent treatment of the A-body target state. We have also ignored the complications due to spin. It is very likely that the projectile-target antisymmetry can be closely approximated by the Takeda-Watson[16] prescription used in NR calculations.

Acknowledgements

It is a pleasure to acknowledge helpful conversations with S. J. Wallace, who first

alerted us to the problems of dissolution singularities. We would also like to thank P. C. Tandy and W. Van Orden for discussions on the subject on various occasions. K. M. M would like to acknowledge the kind hospitality of CEBAF.

This work was supported in part by the Department of Energy, through CEBAF, and by NASA grant NAG-1-477.

References

(1) J. R. Shepard, J. A. McNeil and S. J Wallace, Phys. Rev. Lett.**50**, 1443 (1983). J. A. Tjon and S. J. Wallace, Phys. Rev. C. **36** 1085 (1987).

(2)B. C. Clark, S. Hama, R. L. Mercer, L. Ray and B. D. Serot, Phys. Rev. Lett, 1644 (1983). B. C. Clark, S. Hama, R. L. Mercer, L. Ray and G. W. Hoffmann, Phys. Rev. C **28**, 1421 (1983). L. Ray and G. W. Hoffmann, Phys. Rev. C **31**, 538 (1985). M. V. Hynes, A. Picklesimer, P. C. Tandy and R. M. Thaler, Phys. Rev. Lett. **52**, 978 (1984). M. V. Hynes, A. Picklesimer, P. C. Tandy and R. M. Thaler, Phys. Rev. C **31**, 1438 (1985).

(3)G. E. Brown and D. G. Ravenhall, Proc. R. Soc. London, Sect. A **208** , 552 (1951); J. Sucher, Rep. Prog. Phys. **41**, 1781 (1978); Phys. Rev A **22**, 348 (1980).

(4)K. M. Maung and F. Gross. Bull. Am. Phys. Soc. **32**, 1029 (1987). F.Gross and K. M. Maung Phys. Lett.(accepted for publication)

(5)K. M. Watson, Phys. Rev. **89** 575 (1953).

(6)A. K. Kerman, H. McManus and R. M. Thaler, Ann. Phys. **8**, 511 (1959).

(7)Good accounts on the NR multiple scattering theories can be found in; J. M Einsberg and D. S. Kolton, *Theory of Meson Interactions with Nuclei* (Wiley Interscience, 1980) P. C. Tandy, in *Relativistic Dynamics and Quark-Nuclear Physics*, Edited by M. B. Johnson and A. Picklesimer (Wiley Interscience,1986).

(8)F. Gross, Phys. Rev. C **26**, 2203 (1982).

(9)M. Levy and J. Sucher, Phys. Rev. **186**, 1656 (1969). H. D. I. Abarbanel and C. Itzykson, Phys. Rev. Lett **23**, 53 (1969). S. J. Wallace and J. A. McNeil, Phys. Rev. D **16**, 3565 (1977).

(10)S. J. Wallace (private communication)

(11)Note that the prescription that the $A-1$ cluster be on mass-shell has been given by L. S. Celenza and C. M. Shakin, p 194 *Relativistic Nuclear Physics* , (World Scientific 1986).

(12) F. Gross, Phys. Rev. C **26**, 2226 (1982).

(13) F. Gross, Phys. Rev. **186**, 1448 (1969).

(14)F. Gross, K. M. Maung, T. Tjon, L. W. Townsend and S. J. Wallace. (unpublished)

(15) F. Gross, K. M. Maung, T. Tjon, L. W. Townsend and S. J. Wallace. Phys. Rev. C, **40** R10 (1989).

(16)G. Takeda and K. M. Watson, Phys. Rev. **97**, 1336 (1955).

Figure Captions

Fig 1 The projectile target t-matrix is shown as the sum of all meson exchange processes up to the six order diagrams. The single line represents the projectile and the double line represents the target. The dashed lines are the exchanged mesons. Fig 1a is the one meson exchange term, 1b is the box and 1c the crossed box. In the fourth and higher order diagrams, all possible intermediate target states are summed.

Fig 2 Figure 1b is redrawn by opening up the bubbles at the meson-target vertices. The sum is over the target particles.

Fig 3 Figure 1c is redrawn by opening up the bubbles at the meson-target vertices. The sum is over the target particles.

Fig 4 Figure 1b and 1c are redrawn with explicit labels for the projectile and the target momenta.

Fig 5 The pole structures of the box diagram (4a) and the crossed box diagram (4b) are shown in the complex p_0' plane. The circled dots represent the double meson poles.

Fig 6 The cancellations between the box diagram and the crossed box diagram are shown for $n = 0$. The target mass is taken to be $M_0 = 16m$ where m is the mass of the projectile. See the discussion in the text.

Fig 7 The target mass dependence of the cancellation is shown for $n = 0$. The projectile lab kinetic energy is taken to be 1 GeV. See the discussion in the text.

Fig 8 The cancellations between the box diagram and the crossed box diagram are shown for $n \neq 0$. M_0 is the same as Fig 6 and the excitation energy $\Delta m = m/100$. See the discussion in the text.

Fig 9 Cancellations for $n \neq 0$ shown as a function of excitation energy. See the discussion in the text.

Fig 10 Diagrams which contribute to $\hat{V}$ are shown to fourth order. The first term is the one meson exchange term. The rest of the diagrams are the irreducible diagrams as defined in the text. The dotted circle on a line indicates that the diagram is to be calculated without the on-shell contribution for the projectile(target). These irreducible diagrams as a whole are defined as $\hat{V}'$ in Eq(3.5).

Fig 11 The optimum choice of the propagator g of Eq(3.8). The projectile and the $A-1$ cluster are both on the mass-shell, indicated by a cross. This choice of g minimizes the leading correction term (the second term of Eq(3.10)).

Fig 12 The specator (one particle on-shell) equation is shown diagrammetically. The crosses on a line mean that the particle is on the mass-shell.

Fig 13 This figure represents the quadrature equation Eq(3.14a). The fully off-shell t-matrix $\hat{t}$ is shown by an open oval. The shaded oval is the spectator t-matrix of Eq(3.8). The first term on the RHS is the fully off-shell version of one meson exchange contribution used in Eq(3.8).

=
(a)
(b)
(c)

n
=
i
+
i,i
i
i
+
i,i
i
j

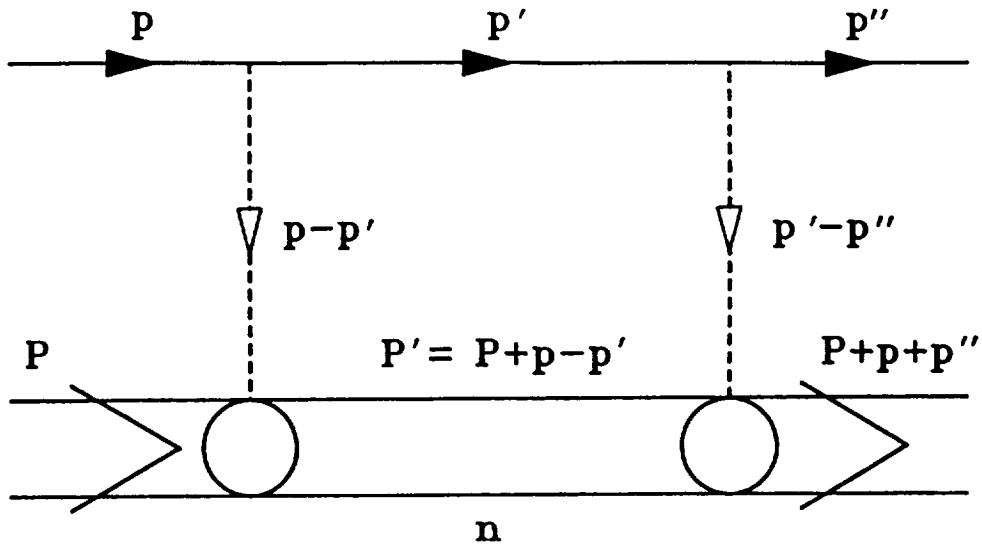

(a)

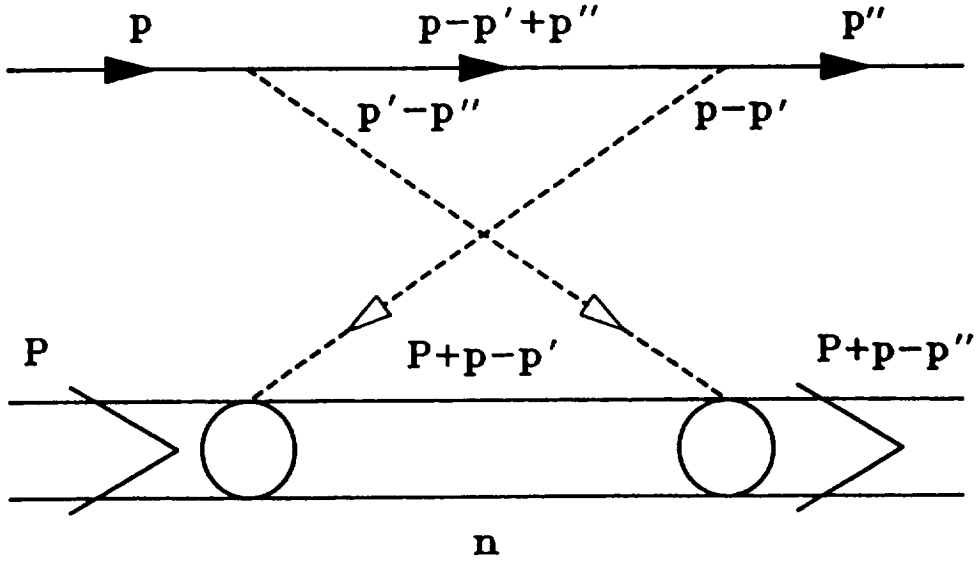

(b)

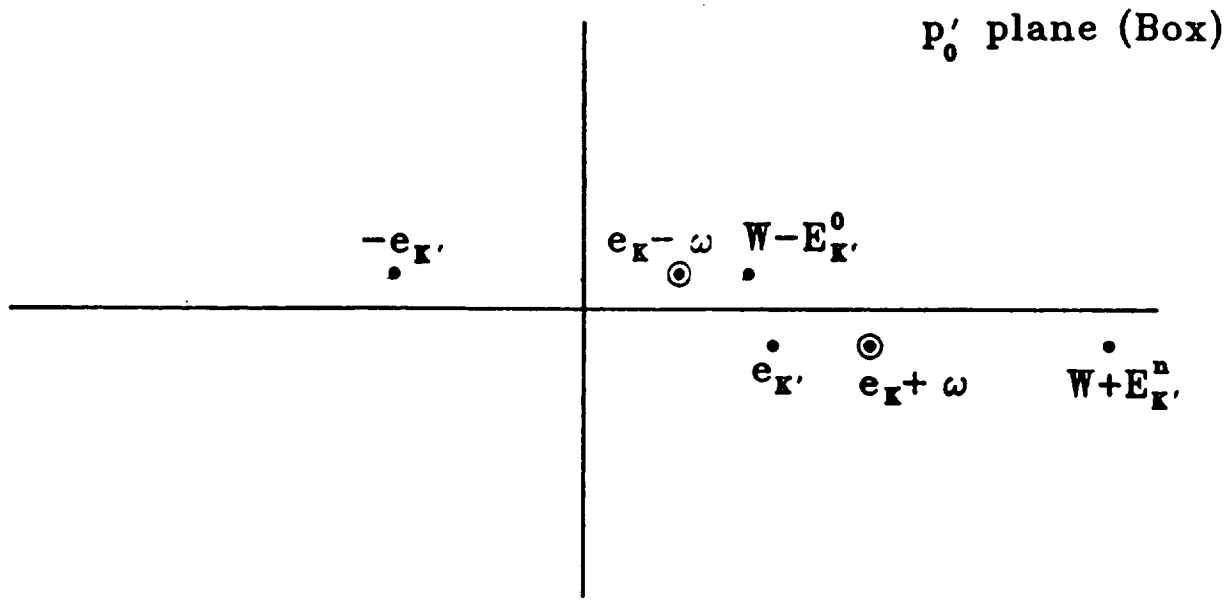
p_0' plane (Box)
$-e_{K'}$
$e_K - \omega$
$W - E^0_{K'}$
$e_{K'}$
$e_K + \omega$
$W + E^n_{K'}$

(a)

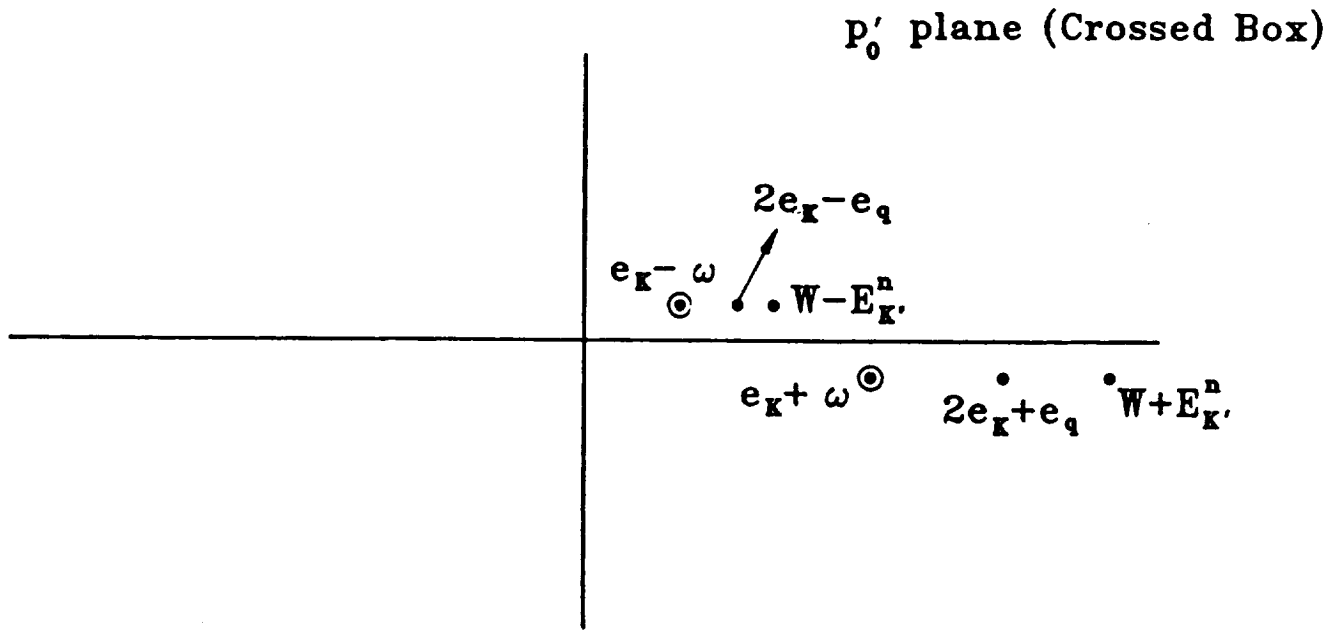
p_0' plane (Crossed Box)
$2e_K - e_q$
$e_K - \omega$
$W - E^n_{K'}$
$e_K + \omega$
$2e_K + e_q$
$W + E^n_{K'}$

(b)

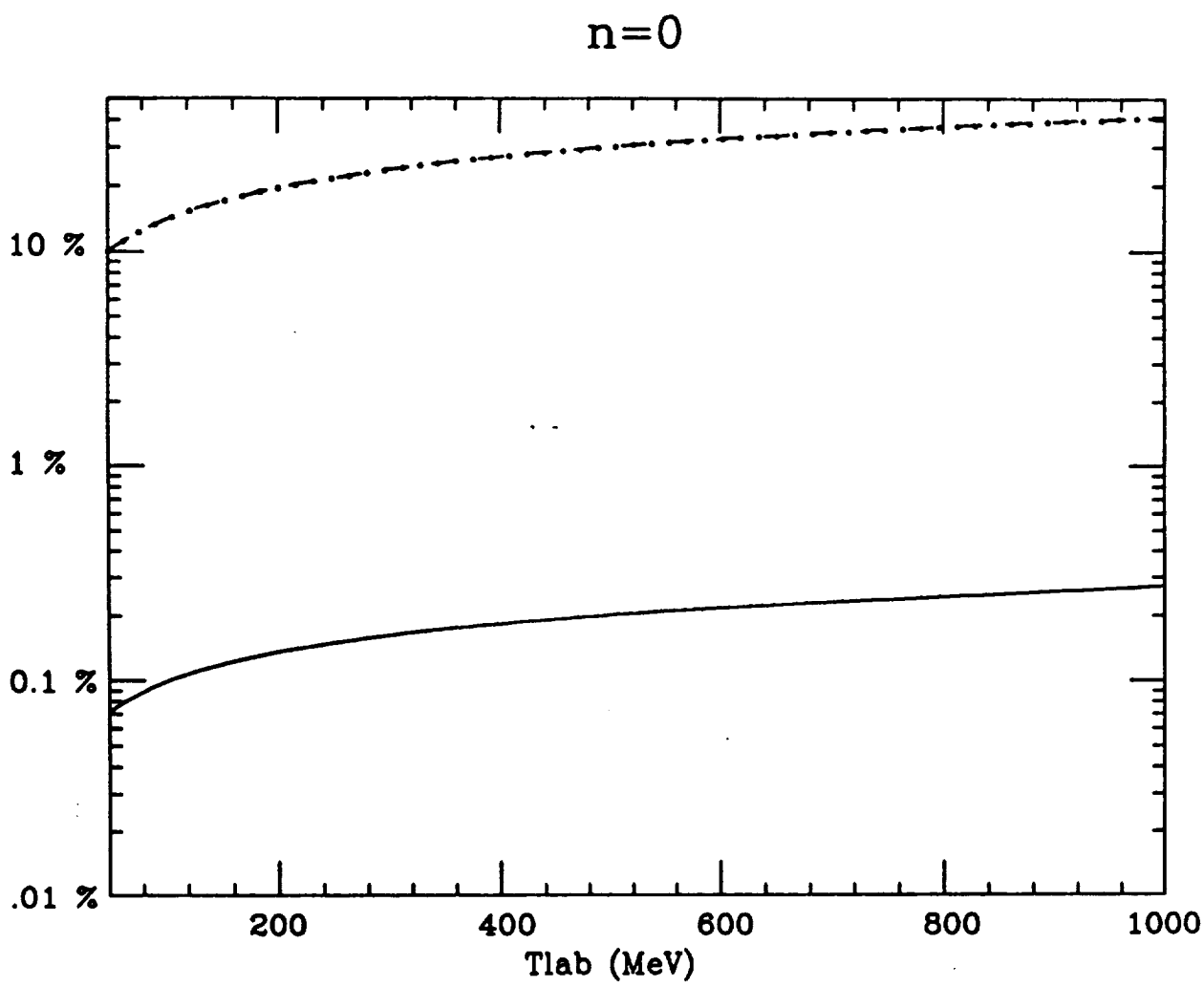
n=0
10 %
1 %
0.1 %
.01 %
200
400
600
800
1000
Tlab (MeV)

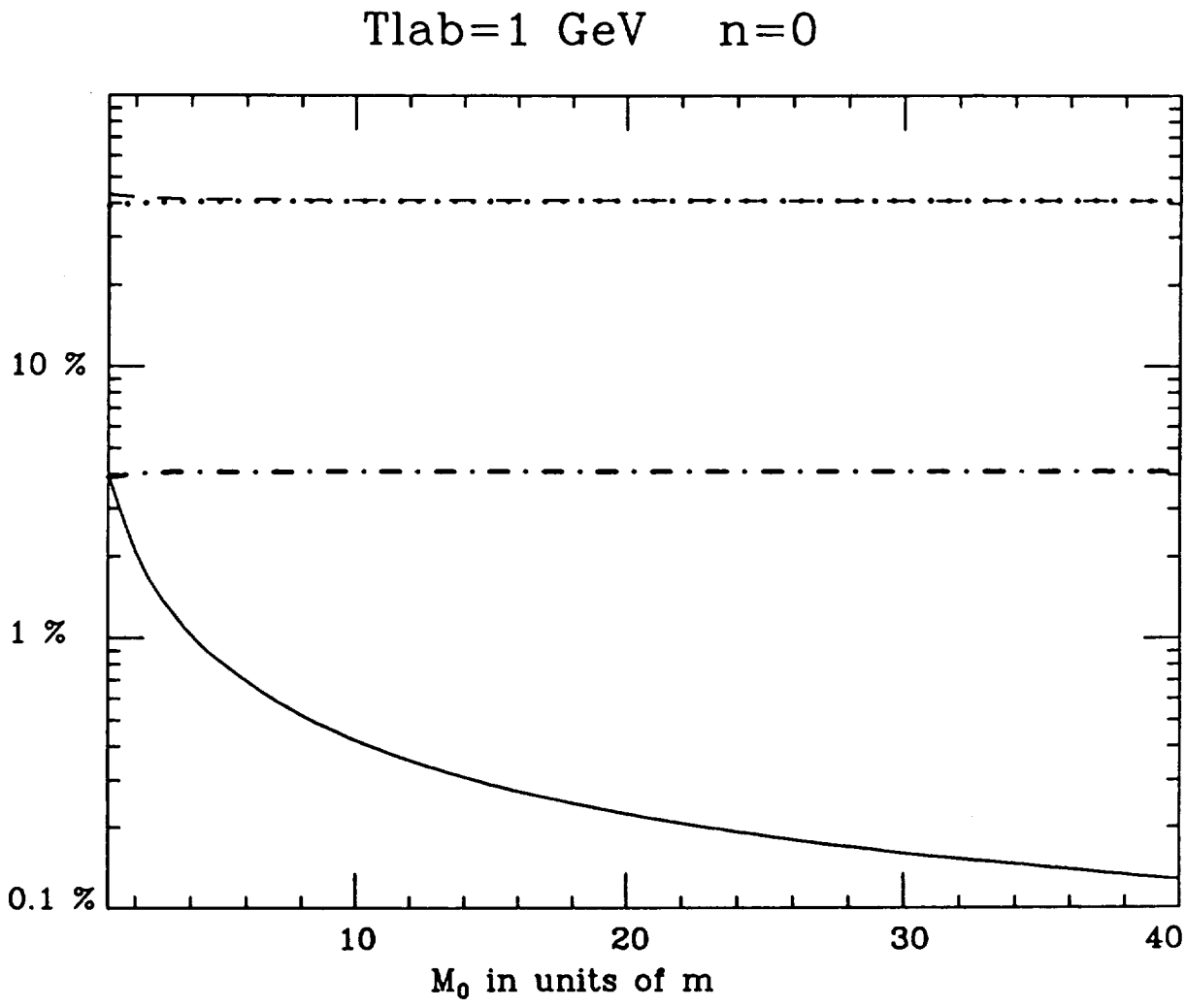
Tlab=1 GeV n=0
10 %
1 %
0.1 %
10
20
30
40
M0 in units of m

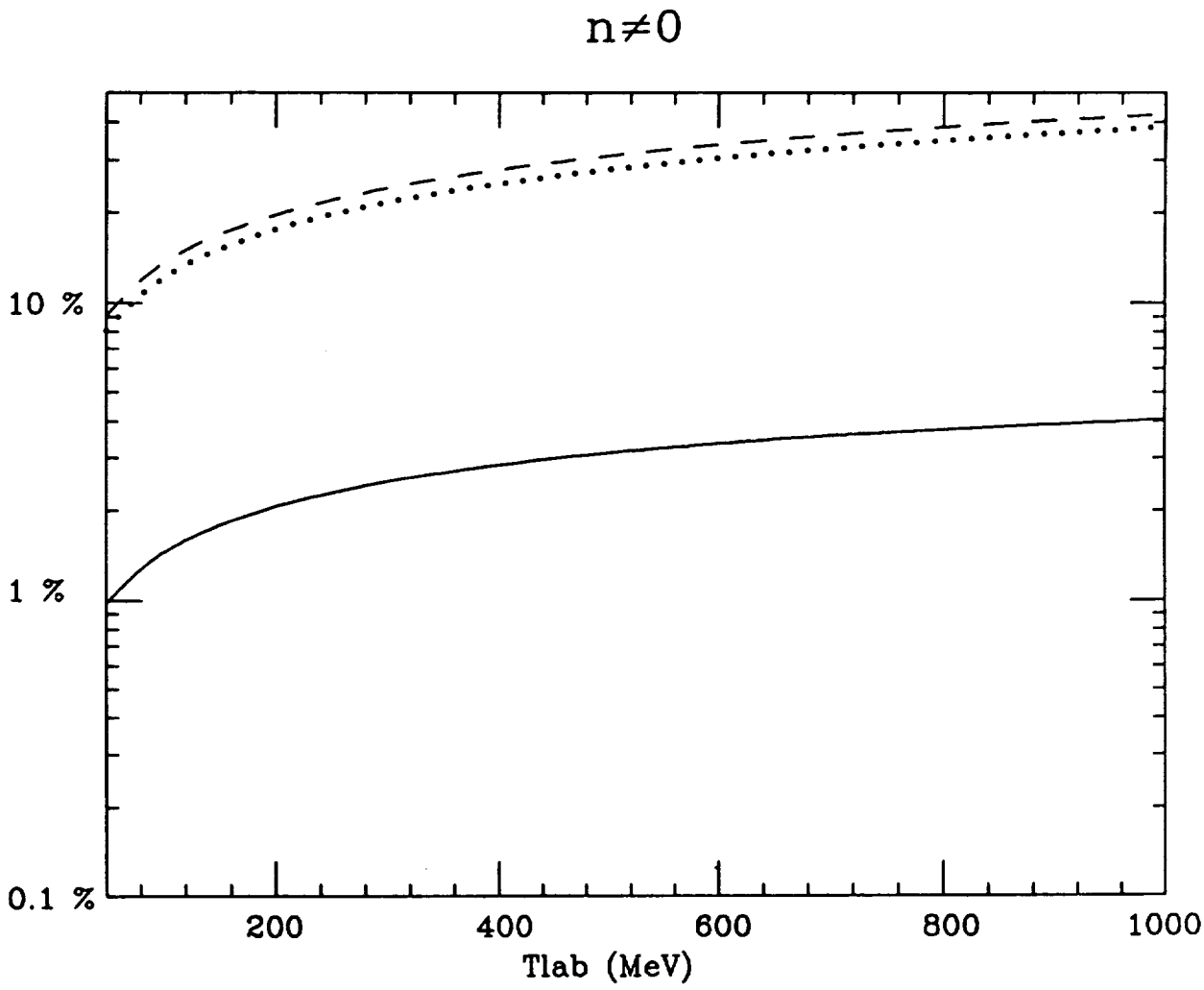
n≠0
10 %
1 %
0.1 %
200
400
600
800
1000
Tlab (MeV)

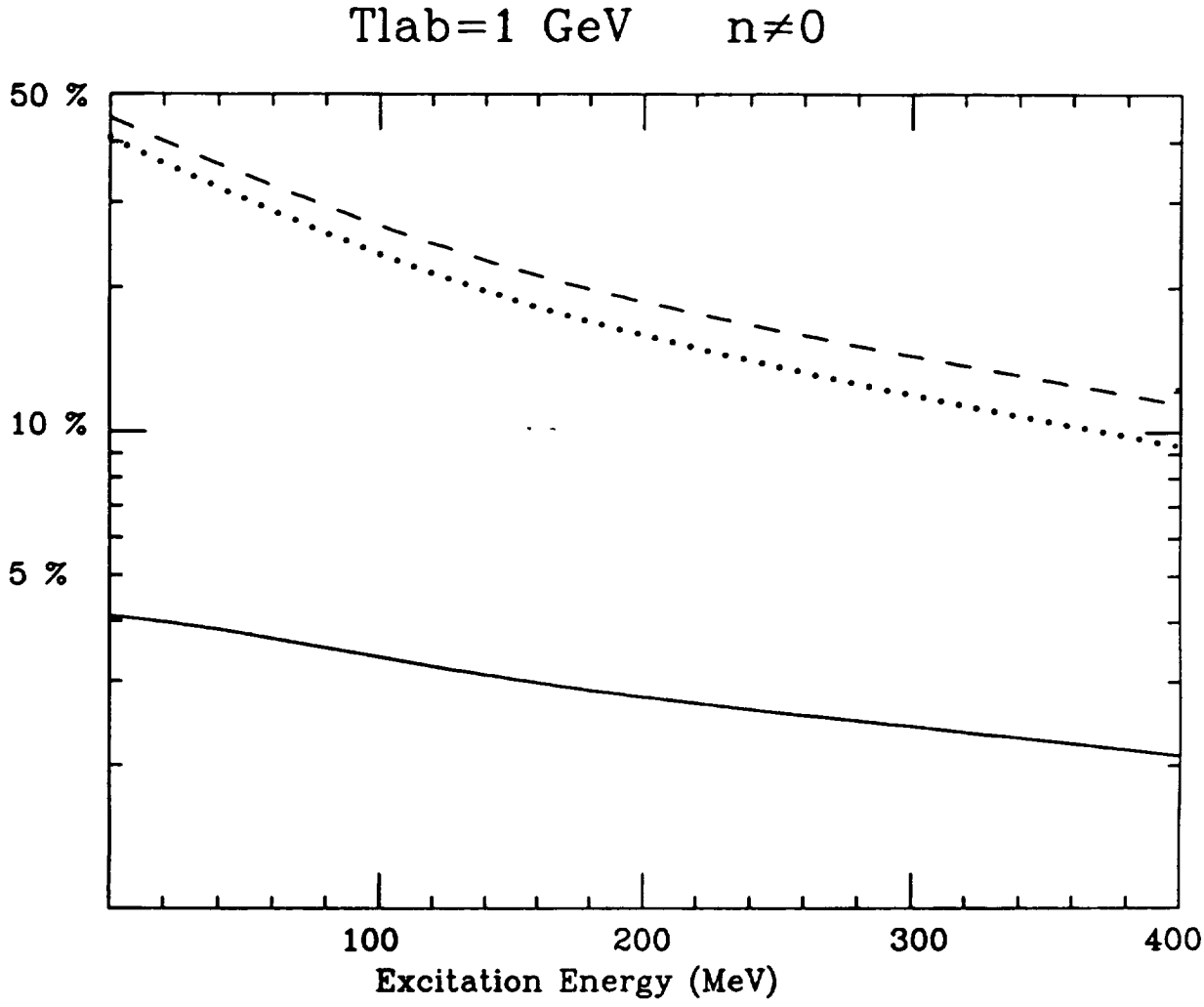
Tlab=1 GeV n≠0
50 %
10 %
5 %
100
200
300
400
Excitation Energy (MeV)

n=0
n
n
n≠0
n≠0

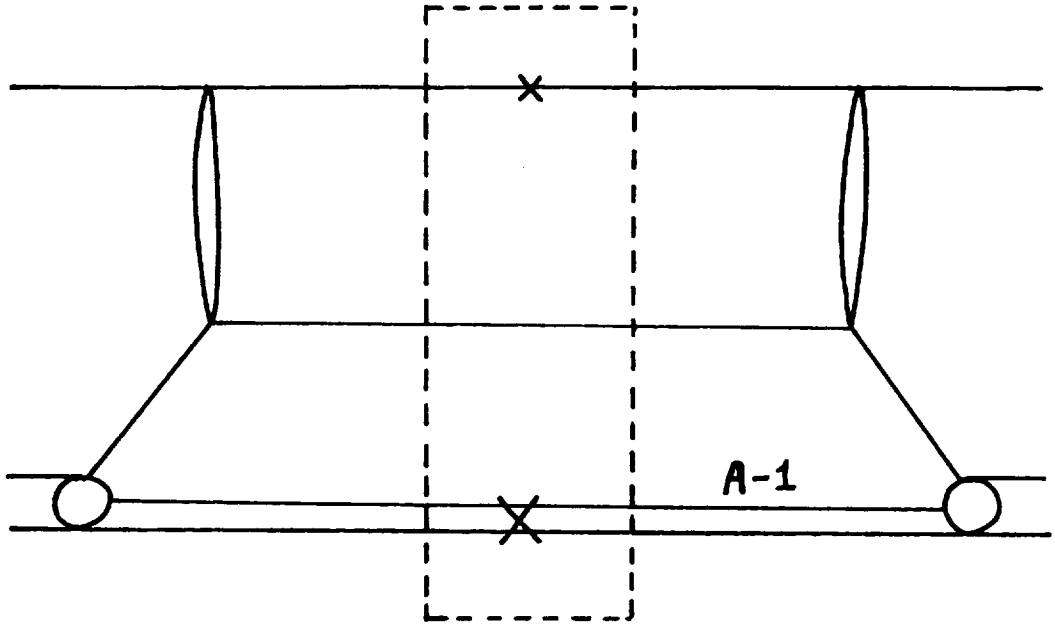

9